Solving the neutron transport equation on unstructured mesh and its application on high-fidelity multi-physics analysis of micro reactors

Tianliang Hu,[1] Duoyu Jiang,[1] Xinyi Zhang,[1] Lipeng Wang,[1] Lu Cao,[1] Huaqi Li,[1] Da Li,[1] and Lixin Chen[1,*]

[1]*Northwest Institute of Nuclear Technology, Xi'an 710024, China*

High-fidelity unstructured mesh based neutron transport method is necessary to accurately model the behavior of micro reactors considering high neutron leakage, the thermal-hydraulics and geometry deformation feedback effects. Based on the MOOSE framework, the multi-group self-adjoint angular flux neutron transport equation is solved. The unstructured mesh modeling capability provides flexibility in representing irregular shapes and boundaries in micro reactors, while the combination of finite element and discrete ordinate methods ensures efficient and accurate solution of the neutron transport equation. The neutron transport solver was then applied for the neutronics analysis of Xi'an Pulsed Reactor, steady-state multi-physics analytical benchmark problem and coupled neutronics/heat transfer/thermal expansion analysis of the Godiva prompt critical transient. The ability of treating the nonlinearity including source-term coupling between different physics, material nonlinearity and geometric nonlinearity are proved in our analysis. Future work will be conducted on more realistic micro reactor designs like heat pipe cooled reactors and gas cooled reactors.

Keywords: Neutron transport; unstructured mesh; micro reactor; MOOSE; multi-physics

I. INTRODUCTION

The International Atomic Energy Agency classifies nuclear reactors with an electric power less than 300MW as small nuclear reactors, and the US Department of Energy recently defined small nuclear reactors with a power level in the MW range as microreactors. Micro reactors have technological advantages such as excellent portability, high thermal efficiency and inherent safety, is attracting more and more attention from the nuclear industry. Their potential lies not only in meeting the increasing global energy needs and combating climate change, but also in being suitable option for providing emergency power supply on land, as well as in deep sea, deep space, and other specific areas in the future[1, 2].

Micro-reactors are known for their compact size and unique design features, such as a control mechanism with rotational control drums. Accurately modeling the high neutron leakage and complex geometry is crucial for simulating the neutronics of advanced micro reactors[3, 4]. Traditional methods like neutron diffusion based nodal methods and finite difference methods are not suitable for this task due to the intricate nature of micro-reactor cores. Instead, a high-fidelity unstructured mesh based neutron transport method allows for a more detailed representation of the core's geometry, leading to more accurate predictions of nuclear reactions and power generation within these small-scale reactors.

Another important part of micro reactor simulation is the necessity of accurately considering the multi-physics coupling effect. Micro reactors are strongly heterogeneous systems and the interactions between neutron transport, thermal heat transfer, and structural mechanics can have significant impacts on each other, leading to complex and interdependent behaviors within the system. Furthermore, the heterogeneity of micro reactors introduces additional challenges in modeling these multi-physics coupling phenomena. The varying scales in space and time of the different physical processes require a comprehensive approach that accounts for their individual characteristics while also capturing their interconnected nature[5, 6]. For the accurate modeling of complex neutronics-thermal-structure mechanics coupling phenomena in micro reactors, it is essential to solve the partial (ordinary) differential equations describing different physics. The key is to solve the nonlinearity caused by multi-physical coupling accurately. For micro reactors, the nonlinearities include (1) the nonlinearity caused by the source-term coupling between different physics: the power distribution calculated from neutronics simulation is heat source of the heat transfer calculation, and the temperature distribution obtained by the heat transfer simulation is the load of the structure mechanics calculation; (2) the material nonlinearity: the neutron cross section in the neutronics calculation, the physical properties in thermal hydraulic and mechanical calculation are influenced by the state parameters such as temperature, density and pressure; (3) the geometric nonlinearity: the deformation of geometry caused by temperature or external load strongly influence the neutron leakage and heat transfer characteristics, thus provide another significant feedback effect. This feedback effect need to be properly handled especially for micro reactors. Traditional analysis tools are developed individually, the mesh is fixed and this effect can only be treated implicitly by modification of atom density.

These two simulation demands have combined to challenge the capabilities of traditional analysis tools. To address these modeling challenges, various efforts have been conducted based on both commercial and open-source multi-physics coupling environments like MOOSE [7], OpenFOAM [8], MFEM [9], and COMSOL [10] in recent years. Tom et al. studied the neutronics characteristics of the CROCUS experimental reactor with the multi-physics coupling analysis code GenFOAM, which was developed based on OpenFOAM, using unstructured mesh to precisely describe the complex geometry of the reactor core [11]. Hu et al. developed

* The name, complete address, telephone number, and e-mail address of the author to whom correspondence and proofs should be sent. E-mail addresses will appear in print and online.

a multi-physics coupling code using the OpenFOAM platform to analyze steady and transient states in fast-spectrum molten salt reactors [12–14]. To investigate the shockwave compression of solid fissile materials, Cervi et al. developed a coupled neutronics-shock physics model using an arbitrary Lagrangian-Eulerian approach, based on the OpenFOAM platform [15]. Wang et al. developed the multi-physics and multi-scheme radiation transport applications Rattlesnake and Griffin on the MOOSE platform [16, 17]. Various reactors, including Empire, SNAP, ATR, NTP, and TREAT, have been analyzed by these codes, proving them to be promising tools for the analysis of advanced micro-reactors [18–22]. To support the modeling and safety analysis of micro-reactors, a code named MEZCAL was developed based on the MFEM library. The code is capable of accurately and effectively solving the multi-group neutron transport equation and is featured by unstructured mesh modeling capability [23]. Wang et al. developed a neutron transport solver using the finite element method within the commercial multi-physics coupling analysis environment COMSOL for hexagonal-z reactor simulation [10]. Jiang et al. developed a three-dimensional space-time kinetics neutron transport code SAAFCGSN based on the MOOSE platform and demonstrated that the SAAFCGSN code achieves high computational accuracy, effectively manages the cusping effect of control rods [24]. The monto carlo method with unstructured mesh capability [25, 26] is also widely adopted in the multi-physics simulation of micro reactors. Mehta et al. demonstrated the significance of capturing multiphysics effects in a hydride-moderated reactor system usning MCNP and Abaqus based Reactor Multiphysics software package [27]. Jaeuk et al. perfomed the multiphysics analysis of the 60-deg symmetrical sector model of the MegaPower three-dimensional core for normal operation and heat pipe–failed conditions using graphics processing unit (GPU)-based continuous-energy Monte Carlo code PRAGMA [28]. Novak et al. implemented an adaptive, on-the-fly mesh-based Monte Carlo geometry algorithm in Cardinal to reduce the barrier-to-entry for high-fidelity multiphysics of reactors [29]. Jiang et al. investigated the coupling calculation of a three-dimensional steady-state neutronics and thermal-hydraulics model for the XAPR by utilizing the Cardinal [30]. Wang et al. studied the thermal deformation simulation, expansion reactivity feedback and density feedback of KRUSTY under the unifiedunstructured mesh using MCNP and Abaqus [31]. Leppanen et al. implementd the multi-physics coupling scheme in Serpent which supports various interface types, including an unstructured OpenFOAM format polyhedral mesh and a special interface type for fuel performance coupling [32]. All these efforts present an alternative and promising way for the high-fidelity analysis of micro-reactors.

In this work, we present an attempt to solve the SAAF (self-adjoint angular flux) neutron transport equation on unstructured mesh based on the MOOSE framework and its application to the multi-physics analysis of micro-reactors. The structure of this paper is as follows: Section 2 presents a detailed description of the physics models, including neutron transport, heat transfer, structural mechanics, and the coupling method. In Section 3, preliminary multi-physics simulations of micro-reactors are demonstrated. Finally, Section 4 summarizes the conclusions.

II. MODELS AND METHODS

A. Unstructured mesh neutron transport method

To accurately estimate the spatial distribution and time evolution of neutron flux and power density in micro reactors, the neutron transport model is adopted in this work. The transient neutron transport equation is a differential-integral equation with seven degrees of freedom, including space, energy, angle, and time. To solve the equation numerically, it needs to be discretized in energy, angle, space, and time. We prefer using discrete ordinates discretization for angular discretization in reactor-like geometries as it provides a good balance between accuracy and efficiency. By combining multi-group and discrete ordinates discretization, we can characterize the neutron transport equation with isotropic scattering as Eq. (1).

$$\begin{aligned}
&\frac{\partial}{\partial t}\left(\frac{\psi_{g,n}(r)}{\upsilon_g}\right)+L\psi_{g,n}(r)+R\psi_{g,n}(r)=S_s\psi(r)+\frac{1}{k_{\text{eff}}}\frac{1}{4\pi}(1-\beta)\chi_{p,g}S_f^p\psi(r)+\frac{1}{4\pi}\sum_{i=1}^{I}\chi_{d,g,i}\lambda_i C_i \\
&\frac{\partial C_i}{\partial t}=-\lambda_i C_i+\beta_i\frac{1}{k_{\text{eff}}}S_f^p\psi(r)=0
\end{aligned} \tag{1}$$

where:

$$\begin{aligned}
&L\psi_{g,n}(r) \\
&=\mathbf{\Omega}_n\cdot\nabla\psi_{g,n}(r) \\
&R\psi_{g,n}(r)=\Sigma_{t,g}\psi_{g,n}(r) \\
&S_s\psi(r)=\sum_{g'=1}^{G}\sum_{n'=1}^{N}\Sigma_{s,g'-g,n'-n}\psi_{g',n'}(r) \\
&S_f^p\psi(r)=\chi_{p,g}\sum_{g'=1}^{G}\nu\Sigma_{f,g}\phi_{g'}
\end{aligned} \tag{2}$$

r is the neutron position defined in the spatial domain; $\mathbf{\Omega}$ is the neutron travel direction; t is the time;g is the index of neutron energy group; ψ is angular neutron flux;k_{eff} is the multiplication factor;υ_g is the speed of neutrons within energy group g; $\Sigma_{t,g}$ is the total cross section for neutrons in energy group g;$\Sigma_{s,g}$ is the scattering cross section for neutrons going from energy group g' to g and from direction n' to n; $\upsilon\Sigma_{t,g'}$ is

the product of the fission cross section and the average number of neutrons generated per fission event for neutrons in energy group g'; $\chi_{p,g}$ is the prompt neutron energy spectrum; $\chi_{d,g,i}$ is the delayed neutron energy spectrum;C_i is the concentration of delayed neutron precursor of group i;λ_i is the decay constant for delayed neutron precursor of group i; β_i is the fraction of neutrons from fission going into delayed neutron precursor group i.

In this study, we use the finite element method to discretize Eqn. (1), which is commonly used in solid mechanics, heat conduction, and other areas. The flexibility of the finite element method in handling unstructured meshes makes it well suited for simulating complex geometries in microreactors. However, directly applying continuous FEM to Eq. (1) can lead to instability due to its representation of a system of hyperbolic PDEs. Continuous finite element method is only stable for elliptic PDEs [23]. Therefore, the SAAF equaiton has been considered in this work. The SAAF equation can be derived by introducing the Auxiliary Flux Equation, it can be defined as:

$$\psi_{g,n}(r) = \frac{1}{\Sigma_{\text{tg}}}(S_s\psi(r) + \frac{1}{k_{\text{eff}}}\frac{1}{4\pi}(1-\beta)\chi_{p,g}S_f^p\psi(r) + \frac{1}{4\pi}\sum_{i=1}^{I}\chi_{\text{d},g,i}\lambda_i C_i - L\psi_{g,n}(r) - \frac{\partial}{\partial t}(\frac{\psi_{g,n}(r)}{\upsilon_g})) \tag{3}$$

The initial stage of the discretization process involves dividing the geometric domain D into separate, non-overlapping elements. Following this, the discretized version of Eq. (1) for the neutron transport equation is multiplied by a test function $v(r)$ and integrated across the problem domain D to derive the weak form:

$$\left(\frac{\partial}{\partial t}(\frac{\psi_{g,n}(r)}{\upsilon_g}),\nu(r)\right) + (L\psi_{g,n}(r),\nu(r)) + (R\psi_{g,n}(r),\nu(r)) = (S_s\psi(r),\nu(r)) + \left(\frac{1}{k_{\text{eff}}}\frac{1}{4\pi}(1-\beta)\chi_{p,g}S_f^p\boldsymbol{\psi}(r),\nu(r)\right) + \left(\frac{1}{4\pi}\sum_{i=1}^{I}\chi_{\text{d},\text{g},i}\lambda_i C_i,\nu(r)\right) \tag{4}$$

$$\left(\frac{\partial C_i}{\partial t},\nu(r)\right) = (-\lambda_i C_i,\nu(r))_i + \left(\beta_i\frac{1}{k_{\text{eff}}}S_f^p\boldsymbol{\psi}(r),\nu(r)\right) \tag{5}$$

(,)represents volume integration.

Using fractional integral and Gaussian theorem, the second term in Eqn. (4) can be translated to:

$$\left(L\psi_{g,n}(r),\nu(r)\right) = \left(L^*\psi_{g,n}(r),\nu(r)\right) + \left\langle\psi_{g,n}(r),\nu(r)\right\rangle \tag{6}$$

<,>represents surface integration.

where

$$(L^*\psi_{g,n}(r),\nu(r)) = -\int_D \boldsymbol{\Omega}_n\cdot\nabla\nu(r)\psi_{g,n}(r)\mathrm{d}r - \int_D L\nu(r)\psi_{g,n}(r)\mathrm{d}r \tag{7}$$

$$\left\langle\psi_{g,n}(r),\nu(r)\right\rangle = \oint_\Gamma \nu(r)\psi_{g,n}(r)\Omega_n\cdot n\mathrm{d}\Gamma \tag{8}$$

Then Auxiliary Flux Equation is inserted into Eq. (7):

$$(L^*\psi_{g,n}(r),\nu(r)) = \int_D \frac{L\nu(r)}{\Sigma_{\text{tg}}}(-S_s\boldsymbol{\psi}(r) - \frac{1}{k_{\text{eff}}}\frac{1}{4\pi}(1-\beta)\chi_{p,g}S_f^p\boldsymbol{\psi}(r) - \frac{1}{4\pi}\sum_{i=1}^{I}\chi_{\text{d},g,i}\lambda_i C_i + L\psi_{g,n}(r) + \frac{\partial}{\partial t}(\frac{\psi_{g,n}(r)}{U_g}))\mathrm{d}r \tag{9}$$

The weak form of the SAAF equation then can be derived as Eqn. (10) and Eqn. (11):

$$\left(\frac{\partial}{\partial t}(\frac{\psi_{g,n}(r)}{\upsilon_g}),\nu(r)+\frac{L\nu(r)}{\Sigma_{\mathrm{t,g}}}\right)+\left(\frac{1}{\Sigma_{\mathrm{t,g}}}L\psi_{\mathrm{g,n}}(r),L\nu(r)\right)+\langle\psi_{\mathrm{g,n}}(r),\nu(r)\rangle+(R\psi_{\mathrm{g,n}}(r),\nu(r))$$
$$=\left(S_s\psi(r),\nu(r)+\frac{L\nu(r)}{\Sigma_{\mathrm{t,g}}}\right)+\left(\frac{1}{k_{\mathrm{eff}}}\frac{1}{4\pi}(1-\beta)\chi_{p,g}S_j^p\psi(r),\nu(r)+\frac{L\nu(r)}{\Sigma_{\mathrm{t,g}}}\right) \tag{10}$$
$$+\left(\frac{1}{4\pi}\sum_{i=1}^{I}\chi_{\mathrm{d},g,i}\lambda_i C_i,\nu(r)+\frac{L\nu(r)}{\Sigma_{\mathrm{t},g}}\right)$$

$$\left(\frac{\partial C_i}{\partial t},\nu(r)\right)=\left(-\lambda_i C_i,\nu(r)\right)_i+\left(\beta_i\frac{1}{k_{\mathrm{eff}}}S_f^p\psi(r),\nu(r)\right) \tag{11}$$

Regarding the boundary conditions, the SAAF equation's boundary condition can be separated into terms for outflow and inflow, which can be represented as follows:

$$\begin{aligned}\left\langle\psi_{_{g,n}}(r),\nu(r)\right\rangle=&\oint_{\Omega_n\cdot n>0}\nu(r)\psi_{_{g,n}}(r)\Omega_n\cdot n\mathrm{d}\Gamma\\&+\oint_{\Omega_n\cdot n<0}\nu(r)\psi_{_{g,n}}(r)\Omega_n\cdot n\mathrm{d}\Gamma\end{aligned} \tag{12}$$

In Eqn.(12), n denotes the unit vector that points outward in the normal direction from the boundary. The vacuum boundary condition is expressed as:

$$\begin{aligned}&\left\langle\psi_{_{g,n}}(r),\nu(r)\right\rangle\\&=\begin{cases}\oint_{\Omega_n\cdot n>0}\nu(r)\psi_{_{g,n}}(r)\Omega_n\cdot n\mathrm{d}\Gamma & \Omega_n\cdot n>0\\0 & \Omega_n\cdot n<0\end{cases}\end{aligned} \tag{13}$$

In this study, we have developed the kernels for each term in Eq. (10) and (11), as well as the boundary conditions for Eqn. (12) and (13) using the MOOSE platform. The MOOSE platform, developed by the Idaho National Laboratory, is an open-source computing platform designed for solving multi-physics numerical problems. It utilizes the finite element method and PJFNK algorithm to efficiently solve partial differential equations in a modular manner. In MOOSE terminology, kernels and boundary conditions are implemented as C++ classes with methods for calculating residual and Jacobian contributions corresponding to specific parts of governing equations. The static neutron transport equation is an eigenvalue problem, which can be solved using the built-in Eigenvalue Executioner in MOOSE. Additionally, various time schemes are available for transient simulations.

B. Heat transfer and structure mechanics model

The Doppler effect and mesh deformation feedback effect are crucial factors that influence the steady and dynamic behavior of micro reactors. These effects can impact the neutron leakage within the reactor, ultimately affecting its performance. To obtain the temperature distribution in micro reactors, it is necessary to apply the energy balance equation with internal heat generation, as shown in Eqn. (14):

$$\rho\mathcal{C}_p\frac{\partial T}{\partial t}=\nabla\cdot(k\nabla T(r,t))+q_{\mathrm{f}}(r,t) \tag{14}$$

The mechanical model solves the conservation of momentum for solid mechanics:

$$-\nabla\bullet\sigma=\rho F \tag{15}$$

We utilize the theory of infinitesimal small strain, which establishes a linear relationship between stress and displacement tensors. This theory is based on the assumption that displacement is significantly smaller than any relevant dimensions, allowing to consider unchanged geometry and constitutive properties of materials at each point in space during deformation. This approach allows for accurate analysis and prediction of material behavior under various loading conditions, providing valuable insights for engineering design and structural analysis. By considering infinitesimally small strains, we can simplify complex problems and make accurate predictions about material behavior without needing to account for large deformations or non-linear effects:

$$\boldsymbol{\varepsilon}=\frac{1}{2}(\nabla_X\boldsymbol{u}+\nabla_X^T\boldsymbol{u}) \tag{16}$$

The symmetric strain tensor and the thermal expansion for isotropic materials are directly linked to the nominal stress tensor σ:

$$\begin{aligned}\sigma_{ij}&=C_{ijkl}\varepsilon_{kl}+\beta_T\Delta T\delta_{ij}\\&=2G\varepsilon_{ij}+\lambda\varepsilon_{kk}\delta_{ij}+\beta_T\Delta T\delta_{ij}\end{aligned} \tag{17}$$

C. Multi-physics coupling method

The equations (1), (14), (15), (16), (17) and the corresponding initial conditions and boundary conditions constitute the multi-physics coupling system. The distribution of neutron flux, power, temperature, displacement and other physical quantities can be obtained by solving the equations. After space and time discretization which are all based on MOOSE platform, the partial differential equations describing neutronics, heat transfer and sturcture mechanics can be

transformed into non-linear equation systems:

$$\begin{bmatrix} K_{11} & K_{12} & K_{13} \\ K_{21} & K_{22} & K_{23} \\ K_{31} & K_{32} & K_{33} \end{bmatrix} \begin{bmatrix} \boldsymbol{\varphi} \\ \boldsymbol{T} \\ \boldsymbol{u} \end{bmatrix} = \begin{bmatrix} \boldsymbol{P}_{\varphi} \\ \boldsymbol{P}_{T} \\ \boldsymbol{P}_{u} \end{bmatrix} \tag{18}$$

Where ϕ, T and u are neutron angular flux, temperature and displacement respectively, K_{ij} and P are problem dependent coupling coefficients.

Methods to solve the multi-physics coupling system can mainly be divided into two categories: strong coupling method and weak coupling method. All the nonlinear equation systems are assembled in a single matrix through a strong coupling way as shown in Eqn. (18) for the strong coupling method. Then discretized nonlinear equations are solved directly and solutions of all the physical quantities are updated at the same time during the iteration. The advantage of the strong coupling method is intuitionistic and simple. Based on MOOSE multi-physical coupling framework, the strong coupling method can be easily realized. At the same time, the strong coupling method can directly use Newton iteration method to update all the solution variables synchronously, and the variables converge at the same time. Moreover, the local convergence rate of Newton iteration method is second order. But the strong coupling method mainly has the following problems: (1) the properties of partial (ordinary) differential equations describing different physics are different, and the direct simultaneous solution of all the equations may lead to large condition number of the matrix, even ill-conditioned, leading to the slow-convergence or even non-convergence of the solutions; (2) Because solving all the nonlinear equations together, the direct simultaneous solution takes up a large amount of memory and computation resource. Generally, it can only be applied to one-dimensional or two-dimensional problems. In the multi-physics coupling analysis of micro reactors, the full three-dimensional strong coupling calculation cannot be realized easily at present; (3) In the calculation of time-dependent problems, there is a problem of time scale inconsistency. The physics with slow change in time may also need to adopt the same time step as the physics with fast change to increase the calculation burden.

Unlike the strong coupling method, the core idea of the weak coupling method is to transform the multi-physics coupling problem into several sub-problems by operator splitting, and the sub-problems are coupled by data transfer. So the solution between different physical models of weak coupling method is completely decoupled as shown in eqn. (19) (20) and (21). By designing different iterative method, the weak coupling method can further be divided into loose coupling method or tight coupling method. The weak coupling method offers the advantage of maximizing the utilization of developed single physics models and codes. The disadvantage is that only the first order convergence can be achieved. For some cases, the convergence rate is slow.

$$K_{11}(T_{fuel}, T_{fluid}) \cdot \varphi = \tilde{P}_{\varphi}(\varphi, T_{fuel}, T_{fluid}) \tag{19}$$

$$\begin{aligned} &K_{22}(\varphi, T_{fuel}, T_{fluid}) \cdot T_{fuel} \\ &= \tilde{P}_{fuel}(\varphi, T_{fuel}, T_{fluid}) \end{aligned} \tag{20}$$

$$K_{33}(T_{fuel}, T_{fluid}) \cdot T_{fluid} = \tilde{P}_{fluid}(T_{fuel}, T_{fluid}) \tag{21}$$

Based on the above methods, a multi-physics coupling analysis code has been developed in this paper. Currently, there are two main strategies for the development of multi-physics coupling code. The traditional strategy is to couple mature and widely validated code together by development of data exchange interface. Since these single-physics codes are often developed with different spatial and temporal numerical discretization methods, the resulted multi-physics code is usually very complex and can only applied for specific cases. The other approach is to develop a multi-physics code based on multi-physics coupling environment with a unified architecture. Representative environment include MOOSE, COMSOL and OpenFOAM. Using a multi-physics coupling environment can unify grid processing, discretization of partial differential equations, solution of linear equation systems, parallel computing, etc., under the framework for all codes developed based on the platform to share. This approach can improve code utilization and avoid redundant development. However, since platforms generally use a single numerical discretization method, the same spatial and temporal numerical discretization methods can only be used for different physical phenomena. For certain specific problems, computational efficiency may be lower than that of the first approach.
In this work, the MOOSE framework is chosen as the development platform. Although MOOSE supports strong coupling method, it often resulted in solve failures from our experience. So in this paper, the majority of our simulations rely on the weak coupling method, with the inclusion of the strong coupling method for thermo-mechanical simulations of Godiva prompt critical transients. The MultiApp and Transfer system in MOOSE allows for weak coupling, enabling the neutronics solver to naturally connect with other physics codes developed on the MOOSE framework, thus enhancing multi-physics capabilities. This integration of different physics codes within the MOOSE framework provides a seamless platform for simulating complex physical phenomena across multiple disciplines.

III. APPLICATION

A. XAPR case

The XAPR is a reactor with light water cooling and graphite reflection. It has two core configurations, one for steady-state operation at 2 MW thermal power and the other for pulsed operation with a peak power of up to 4300 MW. This study focuses on the steady-state operation conditions, as shown in Fig. 1(a). The steady-state core consists of 9 hexagonal rings containing 101 fuel elements, 82 graphite elements, 6 control rod elements, 2 stainless steel elements, 2 running rabbit irradiation tubes, a neutron source element, and a central water chamber. The central water chamber occupies the center of the core with filled water in the middle channels while the graphite reflector elements surround the

perimeter of the core. The standard fuel rod takes up 99 channels while there are two channels for thermometric fuel rods. One channel is used by the neutron source rod and two channels each are occupied by stainless steel elements and running rabbit irradiation tubes. The standard fuel rod consists of a thick stainless-steel cladding, three fuel pellets, three Zr-4 mandrels, and two graphite reflectors, along with upper and lower plugs. The space between the fuel pellet and cladding is filled with 0.1 MPa helium to improve the thermal conductivity of the fuel rod. The XAPR fuel is a uniform combination of enriched uranium and zirconium hydride. Incorporating $UZrH_{1.6}$ in the XAPR leads to a significant immediate negative temperature feedback coefficient, thus providing the core with exceptional inherent safety.

In previous studies, the limitations of either the unstructured-mesh neutron diffusion method[35, 36] or the nodal transport method[38] have been evident in their inability to accurately account for neutron leakage and geometric modeling simultaneously. To address this issue, a detailed unstructured-mesh model was developed for the neutron transport simulation using the MOOSE Reactor module, as depicted in Fig. 1(b). This approach allows for a more comprehensive and precise representation of neutron behavior within complex geometries, leading to improved accuracy in nuclear reactor simulations. By incorporating advanced computational techniques and sophisticated modeling tools, this work aims to overcome the shortcomings of previous methods and provide a more reliable platform for studying micro reactors.

The XAPR core simulation with 224910 elements and S8 level symmetric angular quadrature allows for a detailed analysis of neutron transport within the reactor. Multi-group cross sections for the XAPR reactor model are generated in our previous work and use a 7-group energy structure as shown in Table 1 [38, 39]. In addition, neutron scattering is treated using transport-corrected P0 cross sections, ensuring accurate representation of neutron behavior within the reactor core.

Table 1. Neutron energy group structure

Group	Neutron energy/eV
1	10^7
2	5.00×10^5
3	9.118×10^3
4	4
5	0.625
6	0.14
7	0.058

Comparison is made between the calculated core criticality and the referenced k_{eff} at various control rod positions. The power density distribution of the reactor core can be seen in Fig 2. The core integral parameter k_{eff} at different control rod positions are compared in Table 2. The results from this realistic micro-reactor model indicate that our neutron transport method developed in this paper can properly treat the neutron leakage and complex geometry in micro reactors.

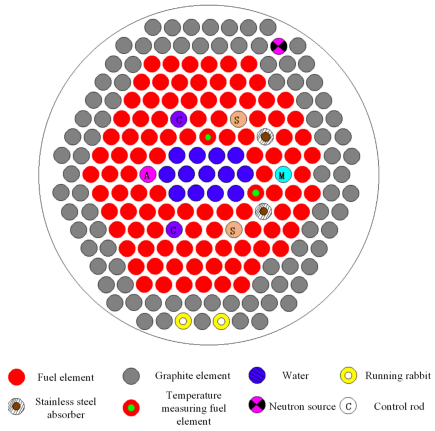

(a)

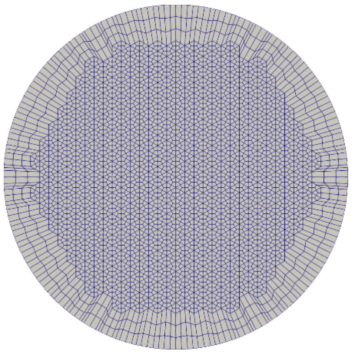

(b)

Fig. 1. 1(a) Radial arrangement of XAPR core 1(b) Mesh adopted in the simulation

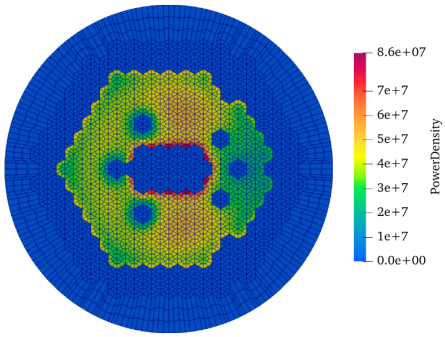

Fig. 2. Power distribution (w/cm^3)

Table 2. Comparison of temperature with various control rod positions

Rod positions	Temperature/ K		Deviation /pcm
	Reference	This work	
D in the bottom	0.99725	0.99955	230
D in the middle	1.00853	1.00615	238
D in the top	1.02584	1.02516	68

B. Multi-physics Analytical benchmark problem

Currently, with the development of computing capabilities, there is an increasing demand for high-fidelity simulation of reactor using multi-physics coupling models. However, there are few relevant benchmark problems and experimental results for netronics/therma/mechanical multi-physics coupling code at present, which limits the verification of related code. In this paper, a one-dimensional nuclear-thermal-mechanical coupling analytical problem proposed by the US Naval Nuclear Laboratory was used to preliminarily verify the multi-physics coupling program based on MOOSE [40]. Although this analytical problem is not based on real reactor design or experimental measurement results, it has the ability to verify the nonlinearity caused by source term coupling in solving multi-physics coupled code as well as material nonlinearity and geometric nonlinearity.

The benchmark problem involves the multiplicative 1-D neutron transport (Eqn. (22) combined with thermal conduction, convection, Doppler broadening (Eqn. (23)), and expansion effects(Eqn. (24)) along the length of the slab. This benchmark presents a highly nonlinear challenge due to the nonlinearity caused by the coupling of source terms between different physics, materials, and geometric deformations.

$$\frac{\mathrm{d}}{\mathrm{d}x}\left[\frac{1}{\Sigma_t(\mathrm{x})}\frac{\mathrm{d}\phi(x)}{\mathrm{d}x}\right]+(\lambda-1)\Sigma_t(\mathrm{x})\phi(x)=0 \tag{22}$$

$$\frac{\mathrm{d}}{\mathrm{d}}\left[k(T)\frac{\mathrm{d}T(x)}{\mathrm{d}x}\right]+q\Sigma_t(x)\phi(x)=0 \tag{23}$$

$$\varepsilon_x=\int_{T_0}^{T}a(T')\mathrm{d}T' \tag{24}$$

The neutron transport model consisting of one-speed neutrons traveling with directions $\mu=\pm1$ in a 1-D slab with initial length L_0, mass density ρ_0, and zero-incident-flux boundary conditions on both sides. For the structure mechanics simulation, the slab is mechanically constrained and perfectly insulated in the transverse dimensions (y and z-axes) but free to expand along the x-axis as the temperature of the slab changes. The thermal expansion coefficient is defined as:

$$\alpha\left(T\right)=\frac{1}{2\sqrt{T_0T}} \tag{25}$$

The steady-state temperature distribution is solved by the thermal conductivity equation. The thermal conductivity is a linear function of temperature as described in Eqn. (26). The boundary condition is convective boundary condition with heat transfer coefficient h at the ends.

$$\kappa(T)=\kappa_0T(x) \tag{26}$$

The neutronics-heat transfer-mechanics coupling simulation is achieved based on the MOOSE MultiApp and Transfer system. The heat transfer simulation is the MasterApp and it has two MultiApps: neutron transport simulation (MultiApp1) and thermal expansion simulation (MultiApp2). The converged solution is achieved by Picard iteration. The power distribution obtained from the neutron transport simulation is transferred to heat conduction simulation, and the temperature distribution obtained from the heat conduction simulation is then used in the thermal stress calculation. The displacement obtained from the thermal stress simulation is further utilized in the heat conduction simulation, which in turn affects the neutron transport simulation. In the simulation, all three models use the same mesh for calculation, so the MultiAppCopyTransfer in MOOSE is adopted for data transfer.

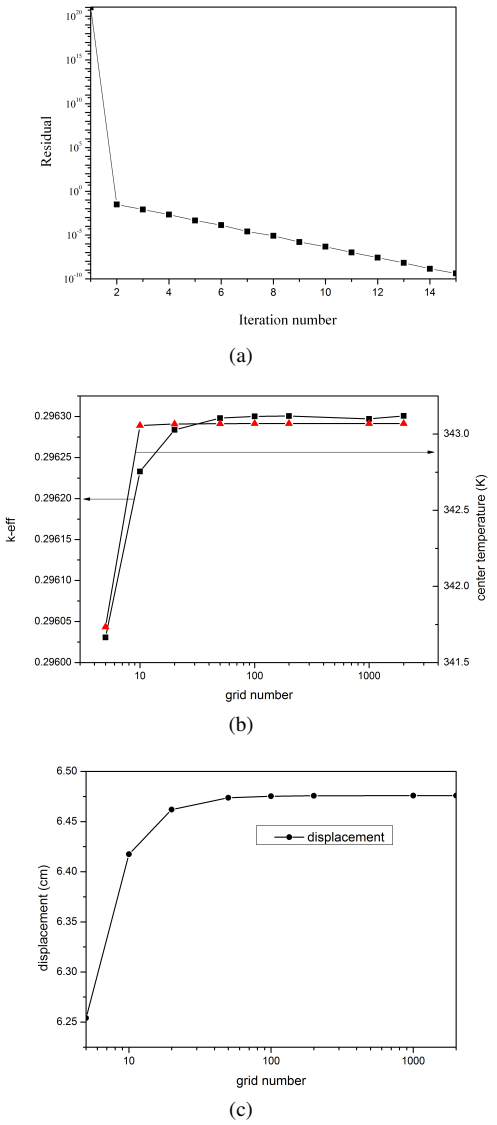

Fig. 3. 3(a) The evolution of residual during the Picard iteration; 3(b) and 3(c) mesh independence study

Because the heat transfer simulation is the MainApp, the initial nonlinear residual of the temperature solution in each Picard iteration step is used as the criterion to judge the convergence of Picard iteration. In the case with mesh number of 100, the residual variation with the Picard iteration number is

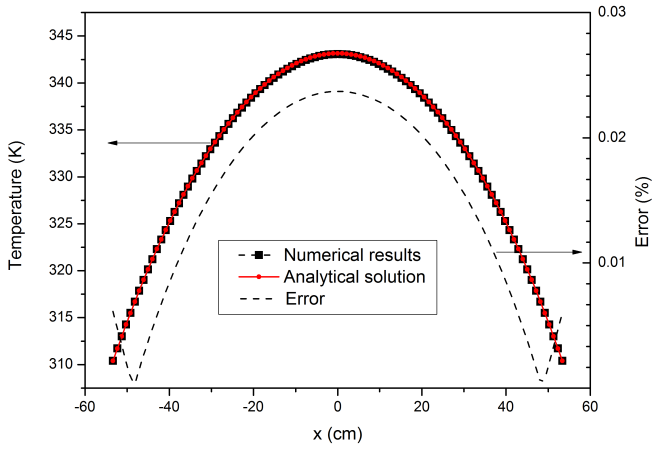

Fig. 4. Temperature comparison between the numerical results and analytical solutions

shown in Fig 3(a).

Firstly, a mesh independence study was performed using different number of elements in the x-direction. In Fig. 3(b) and 3(c), the effective multiplication factor, central temperature($x = 0$) and boundary node displacement are calculated and analyzed. The simulation results converge gradually with the increase of elements number. It can be concluded that the convergent solution can be achieved when the number of grids is 100.

According to the results of mesh independence analysis, the numerical solution with the mesh number of 100 is compared with the analytical solution. The numerical solution of the k_{eff} is 0.29630, the analytical solution is 0.29557 and the derivation is 73pcm. The boundary node displacement is 6.48cm in our numerical simulation, demonstrating strong alignment with the analytical solution of 6.47cm. The central maximum temperature is 343.15K, and the numerical solution is 343.07K. The temperature distribution along the x-direction are compared with the analytical solutions as shown in Fig. 4. The maximum difference is at the center point, less than 0.03%. In general, the numerical results obtained by MOOSE-based multi-physics coupling code are in good agreement with those obtained by analytical solution in neutronics, heat transfer and mechanics. It is proved that the multi-physical coupling strategy can deal with the complex nonlinearity exists in reactor simulation. In micro reactors, the thermal expansion is a significant factor in the feedback mechanism. Changes in the reactor's geometry directly impact the neutron leakage and heat transfer characteristics. The effect of mesh deformation on the neutronics and heat transfer are analyzed as shown in Table 3. The derivations of the our numerical results and the analytical solutions are large under all the three cases, especially in the case that the neutronics simulation does not consider the mesh deformation. In these cases, the deviation of the k_{eff} is large, and maximum difference is 1905 pcm. It is also found that the number of Picard iterations will change significantly if the mesh deformation is not taken into account. Under the conditions of 1 and 3, the number of Picard iterations is reduced to 8, the nonlinear coupling effect is obviously weakened. The number of Picard iterations is reduced by 2 in case 2, which indicates that the main nonlinear effects are caused by the geometric nonlinearity of the neutron transport.

Table 3. Numerical results under different simulation conditions

Simulation condition	k_{eff}	Derivation (pcm)	Central temperature (K)	Derivation (K)	Displacements (cm)	Derivation (cm)
1. Neutronics without mesh deformation	0.27652	1905	346.49	3.34	6.90	0.43
2. Heat transfer without mesh deformation	0.29758	201	338.52	4.55	5.95	0.52
3. Both without mesh deformation	0.27957	1600	341.11	2.04	6.28	0.19

In summary, although the case is not a real micro reactor problem, the analytical solution can effectively test the modeling and computing ability of the existing multi-physical coupling program, especially the capability of treating the geometric nonlinearity.

C. Godiva prompt critical transient problem

The Godiva I is the world's first fast neutron pulse reactor built by LANL. It is an unshielded bare spherical U-235 assembly without reflecting layers. The radius is 8.7407 cm. The critical mass is about 52 kg with density about 18.75 $\mathrm{g/cm^3}$[41]. The fast neutron pulsed reactor can run in the instantaneous supercritical state when the burst pulse occurs. The fission rate increases several orders of magnitude in a few milliseconds, and the relative volume of the core changes, which has the mechanism of thermal expansion and self-extinguishing. Pulse process involves reactor dynamics, unsteady heat transfer, mechanical analysis and coupling process. Therefore, the transient analysis of fast neutron pulse reactor can not only verify the accuracy of neutronics calculation, but also validate the nuclear thermodynamic coupling calculation and the mechanical deformation feedback model.

As shown in Fig. 5, three-dimensional geometry is used for simulation. The heat transfer and mechanical parameters used in the calculation are shown in Table 4 [42]. In heat transfer simulation, the adiabatic boundary condition is adopted

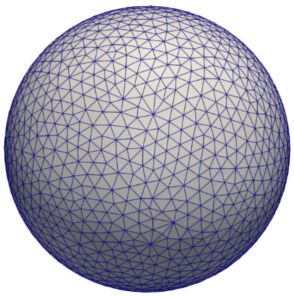

Fig. 5. Mesh in the dynamics simulation

in the surface of the metal sphere. The initial temperature of the sphere is set as uniform temperature at 293.6K. In the dynamic calculation, the surface of the metal sphere is set to free expansion boundary condition, and the initial displacement and velocity are set to 0.

Table 4. Basic parameter of Godiva-I

Parameters	Value
Radius	8.7407 cm
Young's module	2.08×10^{12} g/cm/s^2
Poisson's ratio	0.23
Thermal expansion coefficient	1.39×10^{-5} 1/K
Initial density	18.74 g/cm^3
Heat capacity	0.1177 J/g/K
Thermal conductivity	0.275 W/cm/K

Before the transient simulation, a steady-state neutronics simulation is performed followed by normalizing the reactor core power to 500W. The three-dimensional distribution of power density is shown in Fig. 6 . Notably, the temperature distribution exhibits a similar spatial pattern (with contour shapes mirroring those of the power distribution). The normalized neutron flux acts as the initial condition of the transient calculation. The duration of transient calculation is 0.001 s and the time step is $1 \times 10^{-7}s$ in the simulation.

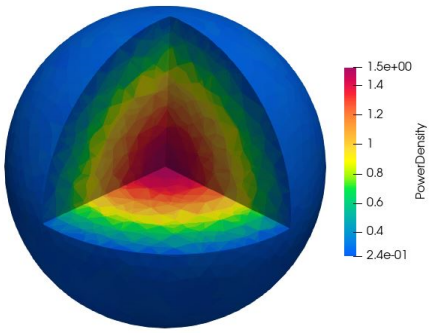

Fig. 6. Three-dimensional distribution of power density (w/cm^3)

Due to the adoption of high enrichment U-235 metal nuclear fuel, the neutron energy spectrum is very hard. And the temperature rise of the system during the transient is relatively small. The Doppler feedback effect on reactivity can be ignored, so only changes in atom density is considered in our simulation. In this paper, the mechanics calculation adopts the infinitesimal small strain theory, and the volume strain of the computational element can be expressed as:

$$\varepsilon_V = \frac{V(t) - V_0}{V_0} = \det(\nabla_X \boldsymbol{u}(t) + \mathbf{I}) - 1 \tag{27}$$

Assuming that the neutron energy spectrum remains unchanged during the transient, the change in neutron macroscopic cross-section is mainly caused by the change in atom density due to the change in the element volume. The method for updating neutron cross sections is shown in the following:

$$\Sigma(t) = \Sigma_0 \frac{V_0}{V(t)} = \Sigma_0 \frac{1}{1 + \varepsilon_V} \tag{28}$$

The explicit temporal coupling between neutronics and thermomechanics is illustrated in Fig. 7. The transient simulation follows this calculation flow at every time step: (1) the internal heat source is calculated by the neutron flux distribution provided by the previous time step; (2) the thermal-mechanics equations are solved by the HeatTransfer and SolidMechanics module in MOOSE framework; (3) the volume strain of each element is calculated according to the nodal displacement according to Eqn. (27). Then the multi-group macro cross-sections are updated according to the atom density change according to Eqn. (28). The displacements are transferred to the meshes of neutronics dynamics calculation for deformation; (4) the neutronics dynamics simulation is performed according to the updated macroscopic cross-section and mesh. The coupled solution of the neutornics dynamics and the therml-mechanics problem are realized by the MultiApp and Transfer systems of MOOSE. The thermo-mechanics solver is used as the MainApp, and the neutronics solver is used as the MultiApp.

Fig. 8(a) and Fig. 8(b) illustrate the changes in power and average temperature over time during a prompt critical transient. With the introduction of step positive reactivity, there is only a slight rise in average temperature as a result of the gradual increase in system power in the initial stage. Then the system power rises rapidly and the temperature increases rapidly. The accumulated fission energy leads to the thermal expansion of uranium metal. The neutron leakage is enhanced due to the deformation and introduces negative reactivity. The core is then in sub-critical state, resulting in a rapid decrease in core power. As a result of the rapid fluctuation in fission power, it is evident that the uranium metal sphere undergoes both compression and expansion, as depicted in Fig. 8(c) and Fig. 8(d), leading to a thermal inertia effect. The oscillation of surface displacement, velocity, and acceleration closely matches the experimental scenario. Since the negative feedback effect was introduced totally by the geometry deformation in this transient, the numerical results prove that method developed in this paper is capable of handling this complicated multi-physics coupling process.

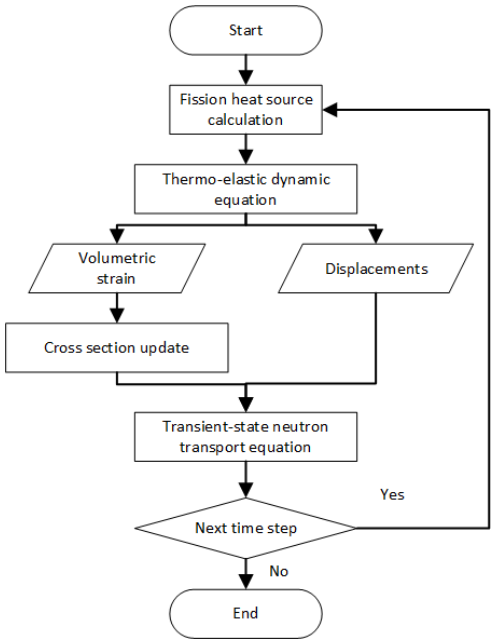

Fig. 7. Flowchart of the multi-physics coupling simulation

IV. SUMMARY AND CONCLUSIONS

The current study involved the development of a second-order SAAF equation-based neutron transport solver within the MOOSE framework. The neutronics solver has the capability of modeling complex geometry as well as the explicit treatment of the mesh deformation, thus provide an efficient tool for the neutronics simulation of advanced micro reactors. Since the neutronics solver is built on MOOSE, it naturally couples to other physics models by either strong coupling or weak coupling method.

As applications, the neutronics solver has been used for the high-fidelity analysis of micro reactors. The XAPR steady-state neutronics simulation was performed in the first place. The numerical results demonstrate that the neutron transport method proposed in this study effectively handles the complex geometry in micro reactors. Then, two multi-physics coupling cases with neutron transport, thermo-mechanics coupling were analyzed based on the method proposed in this work. The ability to handle the nonlinearity caused by source-term coupling, the material nonlinearity and the geometric nonlinearity was proved by both the steady-state and transient-state multi-physics analysis. Our results indicate that the impact of mesh deformation on the reactor core contributes significantly to the behavior of micro reactors. More efforts need to be devoted to the multi-physics modeling of more complex micro reactor designs like heat pipe reactor and gas cooled reactors in the future.

[1] A. Peakman, Z. Hodgson, B. Merk, et al. Advanced micro-reactor concepts [J]. Progress in Nuclear Energy, **107**: 61–70 (2018).

[2] X.Y. Kang, H.Q. Li, S. Chen, et al. Conceptual core schemes and thermal analysis for 5 MWt Heat pipe cooled micro reactor [J]. Modern Applied Physics, **13**(2): 020401 (2022).

[3] Q.Z. Sun, X.J. Liu, X. Chai, et al. A discrete-ordinates variational nodal method for heterogeneous neutron Boltzmann transport problems [J]. Computers & Mathematics with Applications, **170**: 142-160 (2018).

[4] H. Yin, X.J. Liu, T.F. Zhang, et al. An efficient parallel algorithm of variational nodal method for heterogeneous neutron transport problems [J]. Nuclear Science and Techniques, **35**: 69 (2024).

[5] A. G. Mylonakis, M. Varvayanni, N. Catsaros, et al. Multi-physics and multi-scale methods used in nuclear reactor analysis [J]. Annals of Nuclear Energy, **72**: 104–119 (2014).

[6] C. Demaziere. Multi-physics modelling of nuclear reactors: current practices in a nutshell [J]. International Journal of Nuclear Energy Science & Technology, **7**(4): 288–318 (2013).

[7] D. Gaston, C. Newman, G. Hansen, et al. MOOSE: A parallel computational framework for coupled systems of nonlinear equations [J]. Nuclear Engineering and Design, **239**(10): 1768–1778 (2009).

[8] C. Fiorina, I. Clifford, S. Kelm, et al. On the development of multi-physics tools for nuclear reactor analysis based on OpenFOAM®: State of the art, lessons learned and perspectives [J]. Nuclear Engineering and Design, **111604** (2021).

[9] R. A. Robert, MFEM: A modular finite element methods library [J]. Computers & Mathematics with Applications, **81**: 42–74 (2021).

[10] Y.H. Wang, J.C. Chen, D. Li, et al. Simulation of SN transport equation for hexagonal-z reactor using the COMSOL Multi-physics software [J]. Nuclear Engineering and Design, **111604** (2021).

[11] M. Tom, C. Fiorina, H. Mathieu, et al. Investigation and Validation of Unstructured Mesh Methodologies for Modeling Experimental Reactors [J]. Energies, **15**: 1512 (2022).

[12] T.L. Hu, L.Z. Cao, H.C. Wu, et al. Coupled neutronics and thermal-hydraulics simulation of molten salt reactors based on OpenMC/TANSY [J]. Annals of Nuclear Energy, **31**: 107322 (2017).

[13] C.H. Wan, T.L. Hu, L.Z. Cao, et al. Multi-physics numerical analysis of the fuel-addition transients in the liquid-fuel molten salt reactor [J]. Annals of Nuclear Energy, **14**: 104987 (2022).

[14] T.L. Hu, L.Z. Cao, S.H. Yang, et al. Analysis of the thermal feedback effect and nuclides flow effect on the fuel-cycle characteristics of Molten Salt Reactors [J]. International Journal of Energy Research, **45**: 11677–11688 (2021).

[15] E. Cervi, A. Cammi. An Arbitrary Lagrangian-Eulerian, coupled neutronics-shock physics model for the analysis of shock-wave implosion of solid fissile materials [J]. Annals of Nuclear Energy, **141**: 107322 (2020).

[16] Y.Q. Wang, S. Schunert , J. Ortensi, et al. Rattlesnake: A MOOSE-Based Multi-physics Multi-scheme Radiation Transport Application [J]. Nuclear Technology, **1047–1072** (2021).

[17] Y.Q. Wang, C. Lee, Y.S. Jung, et al. Performance Improvements for the Griffin Transport Solvers [R]. US: Idaho National

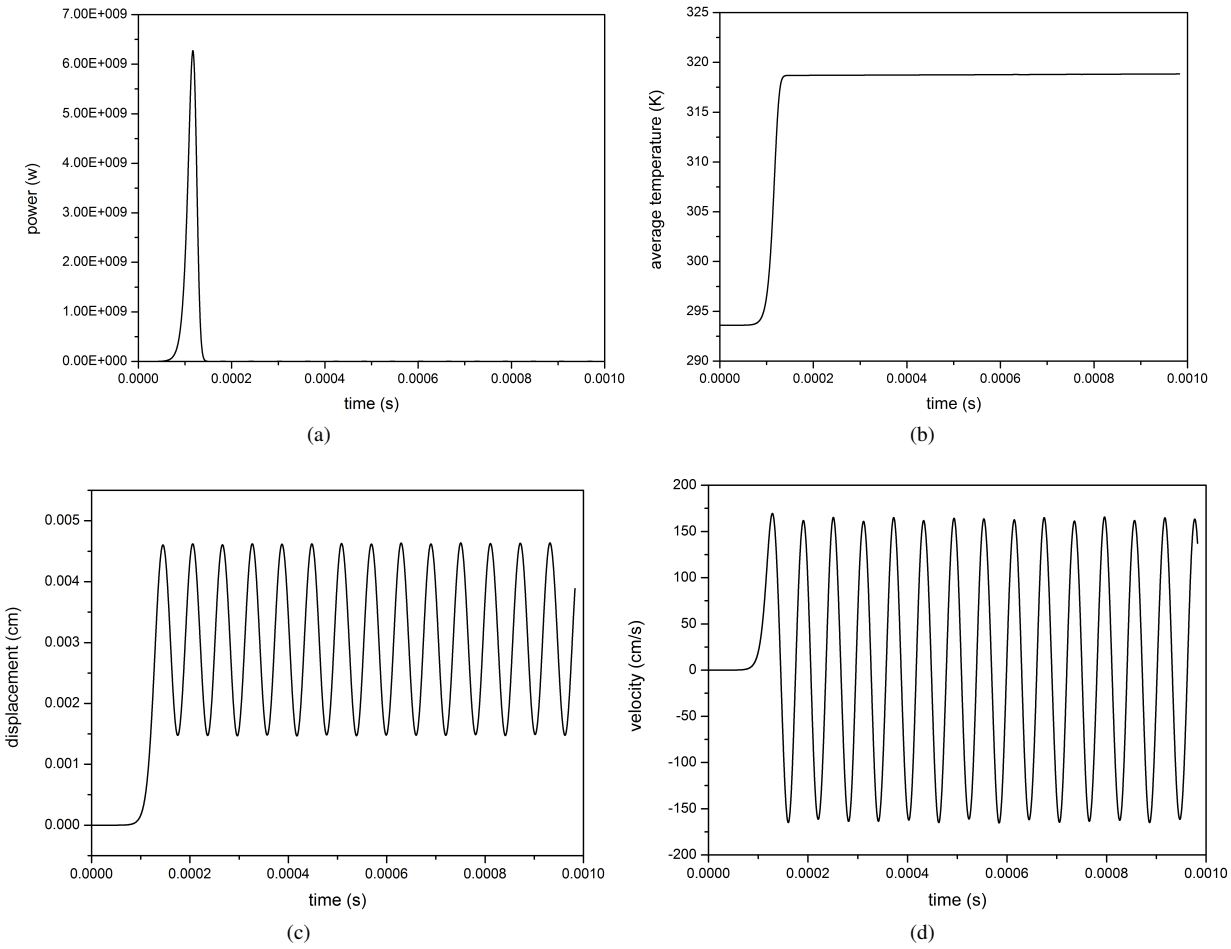

Fig. 8. Time evolution of power(a), temperature(b), surface displacement(c) and surface velocity(d) during the prompt critical transient

Laboratory, 2023.

[18] T. Martin, B. Friederike, J. Matthew, et al. Two-step neutronics calculations with Shift and Griffin for advanced reactor systems [J]. Annals of Nuclear Energy, **173**: 11031 (2022).

[19] H. Khang, M. D. Modeling of the Advanced Test Reactor Using OpenMC, Cubit, and Griffin [R]. US: Idaho National Laboratory, 2023.

[20] O. Havier, A. Benjamin, P. Matthew, et al. Validation of the Griffin application for TREAT transient modeling and simulation [J]. Nuclear Engineering and Design, **385**: 111478 (2021).

[21] N. A. Isaac, G. Sam, L. Ben, et al. Verification of the Serpent-Griffin Workflow using the SNAP 8 Experimental Reactor [R]. US: Idaho National Laboratory, 2023.

[22] M. Vincent, S. Sebastian, T. Stefano, et al. Automated Power-following Control for Nuclear Thermal Propulsion Startup and Shutdown Using MOOSE-based Applications [J]. Progress in Nuclear Energy, **161**: 104710 (2023).

[23] W. C. Dawn, S. Palmtag. Solving the Neutron Transport Equation for Microreactor Modeling Using Unstructured Meshes and Exascale Computing Architectures [J]. Nuclear Engineering and Design, **111604** (2021).

[24] D.Y. Jiang, P. Xu, X.B. Jiang, et al. Application Research on Whole-Core Three-Dimensional Space-Time Kinetics Neutron Transport Code SAAFCGSN [J].Nuclear Power Engineering, **46**(01): 13–23 (2024).

[25] X. Zhang, S.C. Liu, Z.Y. Wang, et al. Development of unstructured mesh tally capability in cosRMC and application to shutdown dose rate analysis [J]. Fusion Engineering and Design, **181**: 113211 (2022).

[26] Z.Y. Wang, S.C. Liu, X.K. Zhang, et al. Research on Monte Carlo Particle Transport Method Directly Using CAD Geometry [J].Atomic Energy Science and Technology, **55**: 88–91 (2021).

[27] V.K. Mehta, J. Armstrong, D.V. Rao, et al. Capturing multiphysics effects in hydride moderated microreactors using MARM [J].Annals of nuclear energy, **172**: 109067 (2022).

[28] J. Lm, M.J. Jeong, J. Choi, et al. Multiphysics Analysis System for Heat Pipe–Cooled Micro Reactors Employing PRAGMA-OpenFOAM-ANLHTP [J].Annals of nuclear energy, **197**(8): 1743–1757 (2023).

[29] A.J. Novak, H. Brooks, P. Shriwise, et al. Monte Carlo multiphysics simulation on adaptive unstructured mesh geometry

[J].Nuclear Engineering and Design, **429**: 113589 (2024).
[30] D.Y. Jiang, P. Xu, T.L. Hu, et al. Coupled Monte Carlo and Thermal-Hydraulics Modeling for the Three-Dimensional Steady-State Analysis of the **'an Pulsed Reactor [J].Energies, **16**(16): 6046 (2024).
[31] L.P. Wang, L. Cao, S. Chen, et al. Study of KRUSTY Thermal Expansion Negative Feedback Calculation Based on Unstructured-Mesh MCNP [J].Nuclear Power Engineering, **44**(02): 286–294 (2024).
[32] J. Leppanen, V. Valtavirta, A. Rintala, et al. Status of Serpent Monte Carlo code in 2024 [J].EPJ Nuclear Sciences Technologies, **11**: 3 (2025).
[33] Q. Zhang, S. Cen. Multiphysics Modeling: Numerical Methods and Engineering Applications: Tsinghua University Press Computational Mechanics Series [M]. Elsevier, 2015.
[34] N. Martin, R. Stewart, S. Bays, et al. A multiphysics model of the versatile test reactor based on the MOOSE framework [J]. Annals of Nuclear Energy, **172**: 109066 (2022).
[35] D.Y. Jiang, P. Xu, T.L. Hu, et al. Transient multi-physics coupling analysis of the Xi'an Pulsed Reactor under pulsed condition [J]. Annals of Nuclear Energy, **200**: 110379 (2024).
[36] T.L. Hu, D.Y. Jiang, X.Y. Zhang, et al. Steady-state analysis of Xi'an Pulse Reactor based on the multi-physics coupling method [J]. Annals of Nuclear Energy, **211**: 110922 (2025).
[37] H.W. Guo, Y.N. Zhu, X.Y. Zhang, et al. Calculation and Experiment of Differential Worth of Adjuster Rod for Xi'an Pulsed Reactor [J]. Modern Applied Physics, **7**(2): 020201 (2016).
[38] X.Y. Zhang, X.B. Jiang, Y.Q. Zheng, et al. Three-dimensional Transient analysis of Xi'an pulsed reactor by the coupled neutronics and thermal-hydraulics code [J]. Annals of Nuclear Energy, **175**: 109254 (2022).
[39] X.Y. Zhang, L.P. Wang, Y.P. Wang, et al. Influence of Depletion on Reactivity Insertion Transients for Xi'an Pulsed Reactor [J]. Nuclear Power Engineering, **44**(5): 30–38 (2023).
[40] D. P. Griesheimer, G. Kooreman. Analytical benchmark solution for 1-D neutron transport coupled with thermal conduction and material expansion [R]. American Nuclear Society-ANS, La Grange Park, IL 60526 (United States), 2022.
[41] R. E. Peterson. Lady Godiva: An unreflected uranium-235 critical assembly, LA-1614 [R]. US: Los Alamos National Laboratory, 1953.
[42] Y.Q. Wang, S. Schunert, J. Ortensi, et al. Demonstration of MAMMOTH Fully Coupled Simulation with the Godiva Benchmark Problem [C]// International Conference on Mathematics & Computational Methods Applied to Nuclear Science & Engineering, 2017.
[43] J.M. Wang, W.F. Liang, S. Chen, et al. Dynamic behavior in fast burst reactor with three-dimensional coupled multiphysics method [J]. Nuclear Engineering and Design, **338**: 16–22 (2018).